COMBINATION OF RCC MPPT AND BACKSTEPPING CONTROLER TO DESIGN A STANDARD CONTINUOUS SOURCE (12V-24V) SUPPLIED BY A PV PANELS

H. Abouobaida, M. Khayat , M. Cherkaoui
Department of Electrical Engineering,
Ecole Mohammadia d'ingénieur, Mohammed V University, Rabat, Morocco
Hassanabouobaida@gmail.com, cherkaoui@emi.ac.ma, elkhayat.med@gmail.com

Abstract: *The present work describes the analysis, modeling and control of a cascade DC-DC power conditioning stage to control a output voltage to supply a DC load systems. To maximize energy extracted from PV generator and control output voltage a RCC MPPT and backstepping controller are designed. The stability of the control algorithm is demonstrated by means of Lyapunov analysis. The achievement of the DC-DC conversion and the efficient PV's energy extraction are validated with simulation results.*

Key Words: *RCC MPPT, backstepping controller.*

1 Introduction

Photovoltaic (PV) is a technology in which the radiant energy from the sun is converted to direct current. The photovoltaic process produces power silently and is completely self-contained, as there are no moving parts. These systems can withstand severe weather conditions including snow and ice. Photovoltaic systems for different applications can be either stand alone or grid connected. In a stand alone system, the load has no connection to the utility grid and often relies on a set of batteries to secure an energy supply at night and other times when the solar panels do not produce electricity. A utility interactive or grid connected system is employed in applications where utility service is already available. In this case, there is no need for battery storage because the power station can be used to supplement photovoltaic generation when the load exceeds the available PV output. The use of photovoltaic as the power source with regulated voltage (12V – 24) is considered as

one of the most important application of PV system. Photovoltaic powered DC system allows to adapte the output voltage to the load even for climatic conditions that may change.

A power conditioning system linking the solar array and the power DC load is needed to facilitate an efficient energy transfer between them, this implies that the power stage has to be able to extract the maximum amount of energy from the PV and to control à voltage of DC load .

In order to extract the maximum amount of energy the PV system must be capable of tracking the solar array's maximum power point (MPP) that varies with the solar radiation value and temperature. Several MPPT algorithms have been proposed, namely, Perturb and Observe (P&O), incremental conductance, RCC algorithms [1]-[2], etc. They differ from its complexity and tracking accuracy but they all required sensing the PV current and/or the PV voltage.

Several controller strategies have been used in the literature, citing the PID that is generally suitable for linear systems, the sliding mode for which the chattering problem, and fuzzy logic adapted to systems without a mathematical model [3].

In this work, the problem of controlling switched power converters is approached using the backstepping technique. While feedback linearization methods require precise models and often cancel some useful nonlinearities, backstepping designs offer a choice of design tools for accommodation of uncertain nonlinearities and can avoid wasteful cancellations. The backstepping approach is applied to a specific class of switched power converters, namely dc-to-dc converters. In the case where the converter model is fully known the backstepping nonlinear controller is shown to achieve the control objectives i.e. input voltage tracking and voltage control of DC load with respect to climate change. The desired array voltage is designed online using a RCC (ripple correlation current) MPP tracking algorithm [4]. The proposed strategy ensures that the MPP is determined, the voltage of DC load is controlled to its reference value and the close loop system will be asymptotically stable. The stability of the control algorithm is analysed by Lyapunov approach. The rest of the paper is organized as follows. The dynamic model of the global system is described in Section II. A backstepping controller is designed along with the corresponding closed-loop error system and the stability analysis is discussed in Section III. In Section IV, a simulation results proves the effectiveness of this approach with constant solar radiation and temperature.

2 MPPT system modelling

The solar generation model consists of a PV array module, dc-to-dc boost converter, dc-to-dc buck converter as shown in Figure 1.

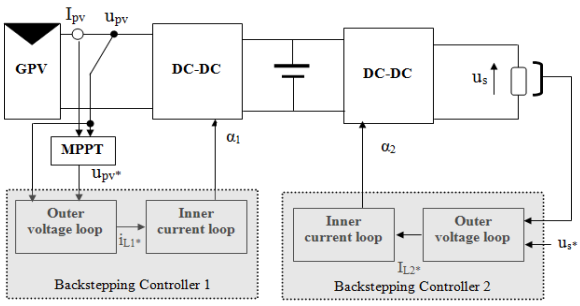

Fig.1. Studied PV system

2.1 PV model

PV array is a p-n junction semiconductor, which converts light into electricity. When the incoming solar energy exceeds the band-gap energy of the module, photons are absorbed by materials to generate electricity. The equivalent-circuit model of PV is shown in Figure 2. It consists of a light-generated source, diode, series and parallel resistances [5].

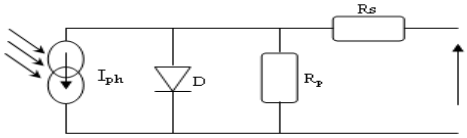

Fig.2. Equivalent model of solar cell

2.2 BOOST converter model

The dynamic model of the power boost converter presented in figure 3 can be expressed by an instantaneous switched model as follows:

$$c_1.\dot{u}_{pv} = I_{pv} - I_{L_1} \quad (1)$$

$$L_1.I_{L_1} = u_{pv} - (1-u_1).u_{dc} \quad (2)$$

Where L_1 and I_{L1} represents the dc-to-dc converter storage inductance and the current across it , u_{dc} is the DC bus voltage and u_1 is the switched control signal that can only take the discrete values 0 (switch open) and 1 (switch closed).

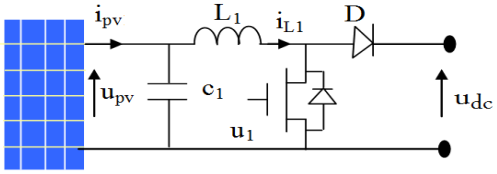

Fig.3. PV array connected to boost converter

Using the state averaging method, the switched model can be redefined by the average PWM model as follows:

$$c_1.\dot{\bar{u}}_{pv} = \bar{I}_{pv} - \bar{I}_{L1} \quad (3)$$

$$L.\dot{\bar{I}}_L = \bar{u}_{pv} - \alpha_1.\bar{u}_{dc} \quad (4)$$

Where α_1 is averaging value of (1- u_1), $\bar{u}_{pv}$ and $\bar{I}_{pv}$ are the average states of the output voltage and current of the solar cell, $\bar{I}_{L1}$ is the average state of the inductor current.

2.3 buck converter model

The power converter here is like buck. It provides power to the DC load with a share of power supplied by the photovoltaic generator and the battery source. This converter accomplish constant voltage (12V or 24V) operation of the DC load. Figure 5 illustrate a buck converter connected to load. Noticing that u_3 stand for the control signal of buck converter, the system can be represented by differential equations:

$$c_2.\dot{u}_s = I_{L2} - \frac{u_s}{R_L} \quad (5)$$

$$L_2.\dot{I}_{L2} = u_2.u_{dc} - u_s \quad (6)$$

Where u_{dc}, u_s designs a battery DC voltage, output buck converter voltage respectively.

And L_2 , I_{L2} and R_L are the dc-to-dc converter storage inductance, the current across it and load resistor. u_2 is the switched control signal that can only take the discrete values 0 (switch open) and 1 (switch closed).

Using the state averaging method, the switched model can be redefined by the average PWM model as follows:

$$c_2.\dot{\bar{u}}_s = \bar{I}_{L2} - \frac{\bar{u}_s}{R_L} \quad (7)$$

$$L_2.\dot{\bar{I}}_{L2} = \alpha_2.u_{dc} - \bar{u}_s \quad (8)$$

Where α_2 is averaging value of u_2 and $\bar{u}_s$ is the average states of the output.

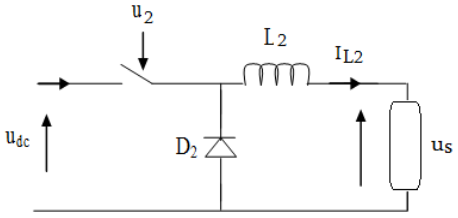

Fig.4. buck converter connected to DC motor

2.4 RCC MPPT

RCC (Ripple correlation control) makes use of ripple to perform MPPT. RCC correlates the time derivative of the time-varying PV array power $\dot{P}$ with the time derivative of the time-varying PV array current $\dot{I}$ or voltage $\dot{V}$ to drive the power gradient to zero, thus reaching the MPP. if V or I is increasing ($\dot{V} > 0$ or $\dot{I} > 0$) and P is increasing ($\dot{P} > 0$), then the operating point is below the MPP ($V < V_{MPP}$ or $I < I_{MPP}$). On the other hand, if V or I is increasing and P is decreasing ($\dot{P} < 0$), then the operating point is above the MPP ($V > V_{MPP}$ or $I > I_{MPP}$). Combining these observations, we see that $\dot{P}.\dot{V}$ or $\dot{P}.\dot{I}$ are positive to the left of the MPP, negative to right of the MPP, and zero at the MPP [1]. When the power converter is a boost converter, increasing the duty ratio increases the inductor current, which is the same as the PV array current, but decreases the PV array voltage [2]. Therefore, the duty ratio control input is :

$$d(t) = -k.\int \dot{P}.\dot{V}.dt \quad \text{or} \quad d(t) = -k.\int \dot{P}.\dot{I}.dt \quad (9)$$

In this paper we used the RCC MPPT to generate the reference voltage of the photovoltaic source such as:

$$u_{pv}^* = k_1.\int \dot{p}_{pv}.\dot{u}_{pv}.dt \quad (10)$$

Where p_{pv} and u_{pv} are respectively a power and voltage of solar panels. k_1 is a constant factor.

3 Nonlinear controller Design

Two main objectives have to be fulfilled in order to transfer efficiently the photovoltaic generated energy into the DC load are tracking the PV's maximum power point (MPP) and control output voltage of DC load. Figure 5 shows the control scheme used to accomplish the previous objectives.

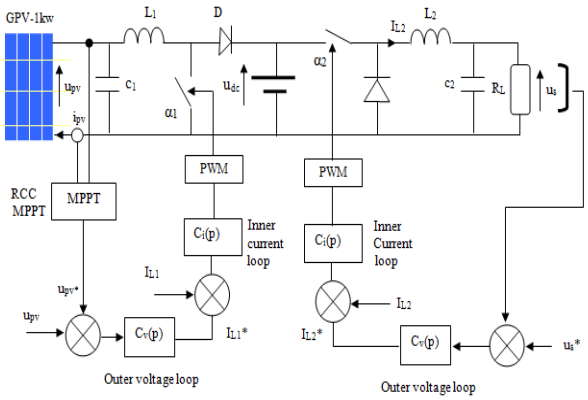

Fig.5 Control scheme for boost converter and buck converter

3.1 Backstepping controller to extract maximum power

The boost converter is governed by control signal α_1 generated by a backstepping controller that allow to extract maximum of photovoltaic generator control by regulating the voltage of the photovoltaic generator to its reference provided by RCC MPPT algorithm.

Step 1. Let us introduce the input error:

$$e_1 = \bar{u}_{pv} - u_{pv}^* \tag{11}$$

Deriving e_1 with respect to time and accounting for (3), implies:

$$\dot{e}_1 = \dot{\bar{u}}_{pv} - \dot{u}_{pv}^* = \left(\frac{\bar{I}_{pv}}{c_1} - \frac{\bar{I}_{L_1}}{c_1} \right) - \dot{u}_{pv}^* \tag{12}$$

In equation (12), i_{L1} behaves as a virtual control input. Such an equation shows that one gets $\dot{e}_1 = -k_1.e_1$ ($k_1>0$ being a design parameter) provided that:

$$I_{L_1} = k_1.c_1.e_1 + \bar{I}_{pv} - c_1.\dot{u}_{pv}^* \tag{13}$$

As i_{L1} is just a variable and not (an effective) control input, (12) cannot be enforced for all $t \geq 0$. Nevertheless, equation (14) shows that the desired value for the variable i_{L1} is:

$$I_{L_1}^* = k_1.c_1.e_1 + I_{pv} - c_1.\dot{u}_{pv}^* \tag{14}$$

Indeed, if the error:

$$e_2 = I_{L_1} - I_{L_1}^* \tag{15}$$

vanishes (asymptotically) then control objective is achieved i.e. $e_1 = u_{pv} - u_{pv}^*$ vanishes in turn. The desired value I_{L1}^* is called a stabilization function.

Now, replacing i_{L1} by $(e_2 + I_{L1}^*)$ in (12) yields:

$$\dot{e}_1 = \left(\frac{\bar{I}_{pv}}{c_1} - \frac{\bar{I}_{L_1}^* + e_2}{c_1} \right) - \dot{u}_{pv}^* \tag{16}$$

which, together with (14), gives:

$$\dot{e}_1 = -k_1.e_1 - \frac{e_2}{c_1} \tag{17}$$

Step 2. Let us investigate the behavior of error variable e_2.

In view of (4) and (15), time-derivation of e_2 turns out to be:

$$\dot{e}_2 = \dot{\bar{I}}_{L_1} - \dot{I}_{L_1}^* = \left(\frac{\bar{u}_{pv}}{L_1} - \frac{\alpha_1.\bar{u}_{dc}}{L_1} \right) - \dot{I}_{L_1}^* \tag{18}$$

From (14) one gets:

$$\dot{I}_{L_1}^* = k_1.c_1.\dot{e}_1 + \dot{\bar{I}}_{pv} - c_1.\ddot{u}_{pv}^* \tag{19}$$

which together with (18) implies:

$$\dot{e}_2 = \frac{\bar{u}_{pv}}{L_1} - \frac{\alpha_1.\bar{u}_{dc}}{L_1} - k_1.c_1.\dot{e}_1 - \dot{\bar{I}}_{pv} + c_1.\ddot{u}_{pv}^* \tag{20}$$

In the new coordinates (e_1,e_2), the controlled system in (3) and (4) is expressed by the couple of equations (17) and (20). We now need to select a Lyapunov function for such a system. As the objective is to drive its states (e_1,e_2) to zero, it is natural to choose the following function:

$$v_1 = \frac{1}{2}.e_1^2 + \frac{1}{2}.e_2^2 \tag{21}$$

The time-derivative of the latter, along the (e_1,e_2)-trajectory, is:

$$\dot{v} = e_1.\dot{e}_1 + e_2.\dot{e}_2$$

$$\dot{v} = -k_1.e_1^2 - k_2.e_2^2$$

$$-e_2.\left[-\frac{\bar{u}_{pv}}{L_1} - \frac{\alpha_1.\bar{u}_{dc}}{L_1} + k_1.c_1.\dot{e}_1 + \frac{e_1}{c_1} + \dot{\bar{I}}_{pv} - c_1.\ddot{u}_{pv}^* - k_2.e_2 \right] \tag{22}$$

where $k_2>0$ is a design parameter and $\dot{e}_2$ is to be replaced by the right side of (20). Equation (22) shows that the equilibrium $(e_1,e_2)=(0,0)$ is globally asymptotically stable if the term

between brackets in (22) is set to zero. So doing, one gets the following control law:

$$\alpha_1 = \frac{L_1}{\bar{u}_{dc}}\left[\frac{\bar{u}_{pv}}{L_1} - \frac{e_1}{c_1} + k_2.e_2 - k_1.c_1.\dot{e}_1 - \dot{\bar{I}}_{pv} + c_1.\ddot{u}_{pv}^*\right] \quad (23)$$

Proposition 1: Consider the control system consisting of the average PWM Boost model (3)-(4) in closed-loop with the controller (23), where the desired input voltage reference u_{pv}^* is sufficiently smooth and satisfies $u_{pv}^* > 0$. Then, the closed loop system errors (e_1,e_2) achieve globally asymptotically stable.

3.2 voltage controller design

This controller consists of an inner current loop and an outer voltage loop. The inner current loop is responsible to regulate the current of storage inductance in buck converter. The outer loop assures a steady-state control a output voltage.

Step 1. Let us introduce the input error :

$$e_3 = \bar{u}_s - u_s^* \quad (24)$$

Where u_s^* is a derivable reference signal of output voltage of DC load. Deriving e_3 with respect to time and accounting for (7) implies:

$$\dot{e}_3 = \dot{\bar{u}}_s - \dot{u}_s^* = \frac{\bar{I}_{L2}}{c_2} - \frac{\bar{u}_s}{R_L.c_2} \quad (25)$$

Where I_{L2} is a virtual control input. Such an equation shows that one gets $\dot{e}_3 = -k_3.e_3$ ($k_3>0$ being a design parameter) provided that:

$$I_{L2}^* = \frac{\bar{u}_s}{R_L} - k_3.e_3.c_2 \quad (26)$$

As I_{L2}^* is just a variable (not effective) control input, equation (26) cannot be enforced for all $t \geq 0$. Indeed, a new error is introduced:

$$e_4 = \bar{I}_{L2} - I_{L2}^* = \bar{I}_{L2} - \left[\frac{\bar{u}_s}{R_L} - k_3.e_3.c_2\right] \quad (27)$$

vanishes (asymptotically) then control objective is achieved i.e. $e_3 = \bar{u}_s - u_s^*$ vanishes in turn. The desired value I_{L2}^* is called a stabilization function.

Now, replacing I_{L2} by $(i_{L2}^* + e_4)$ in (25) yields:

$$\dot{e}_3 = \frac{i_{L2}^* + e_4}{c_2} - \frac{u_s}{R_L.c_2} \quad (28)$$

which, together with (26), gives:

$$\dot{e}_3 = -k_3.e_3 + \frac{e_4}{c_2} \quad (29)$$

Step 2. Let us investigate the behavior of error variable e_4.

In view of (8), time-derivation of e_4 turns out to be:

$$\dot{e}_4 = \dot{I}_{L2} - \dot{I}_{L2}^* = \left(\frac{\alpha_2.\bar{u}_{dc}}{L_2} - \frac{\bar{u}_s}{L_2}\right) - \dot{I}_{L2}^* \quad (30)$$

From (26) one gets:

$$\dot{I}_{L2}^* = \frac{\dot{\bar{u}}_s}{R_L} - k_3.\dot{e}_3.c_2 \quad (31)$$

Substituting (31) in (30) implies:

$$\dot{e}_4 = \frac{\alpha_2.\bar{u}_{dc}}{L_2} - \frac{\bar{u}_s}{L_2} - \left(\frac{\dot{\bar{u}}_s}{R_L} - k_3.\dot{e}_3.c_2\right) \quad (32)$$

In the new coordinates (e_3,e_4), the controlled system is expressed by the couple of equations (36) and (39). We now need to select a Lyapunov function for such a system. As the objective is to drive its states (e_3,e_4) to zero, it is natural to choose the following function:

$$v_2 = \frac{1}{2}.{e_3}^2 + \frac{1}{2}.{e_4}^2 \quad (33)$$

The time-derivative of the latter, along the (e_3,e_4) trajectory is:

$$\dot{v} = e_3.\dot{e}_3 + e_4.\dot{e}_4$$

$$\dot{v} = -k_3.{e_3}^2 - k_4.{e_4}^2$$

$$+e_4.\left[\frac{\alpha_2.\bar{u}_{dc}}{L_2}-\frac{\bar{u}_s}{L_2}-\frac{\dot{\bar{u}}_s}{R_L}+k_3.e_3.c_2+k_4.e_4+\frac{e_3}{c_2}\right] \quad (34)$$

where $k_4>0$ is a design parameter. Equation (34) shows that the equilibrium $(e_3,e_4)=(0,0)$ is globally asymptotically stable if the term between brackets in (34) is set to zero. So doing, one gets the following control law:

$$\alpha_2=\frac{L_2}{\bar{u}_{dc}}.\left[\frac{\bar{u}_s}{L_2}-\frac{\dot{\bar{u}}_s}{R_L}-k_3.\dot{e}_3.c_2-\frac{e_3}{c_2}-k_4.e_4\right] \quad (35)$$

Proposition 2: Consider the control system consisting of the average PWM Buck model in closed-loop with the controller (35), where the desired DC output voltage reference u_s* is sufficiently smooth. Then, the equilibrium $i_{L2}\to i_{L2}*$, $\bar{u}_s\to u_s*$ and $\alpha_2\to\alpha_{20}$ is asymptotically stable where :

$$\alpha_{20}=\frac{\bar{u}_s}{\bar{u}_{dc}} \quad (36)$$

4 Simulation results

The PV model, boost, buck DC-DC converter and backstepping controller are implemented in Matlab/Simulink as illustrated in Figure 5. In the study, RSM-60 PV module has been selected as PV power source in cooperation with battery source, and the parameter of the PV source are chosen to deliver maximum 1kW of power generated by connecting 16 module of RSM-60 parallely. The specification of the system and PV module are respectively summarized in the following table:

TABLE 1
MAIN CHARACTERISTICS OF THE PV GENERATION SYSTEM

Maximum power	Output voltage at P_{max}	Open-circuit voltage	Short current circuit
60w	16v	21.5v	3.8A

TABLE 2
CONTROL PARAMETERS USED IN THE SIMULATION

Parameters	Value	unit
c_1	220	µF
c_2	470	µF
L_1	0.002	H
L_2	0.001	H
u_{dc}	100	V

TABLE III
PARAMETERS USED IN BACKSTEPPING CONTROLLER 1 AND 2

Parameters	Value	unit
k_1	100	
k_2	1000	
k_3	0.1	
k_4	10	

A Matlab® simulation of the complete system with the backstepping controller and the MPPT algorithm has been carried out using the following parameters:

- Switching frequency = 25kHz
- Irradiation = 1000W/m^2
- Temperature T=25°C

The studied PV system is evaluated on two aspects: the first one to extract the maximum power on the PV panels) when the solar radiation and temperature are constant. The second one is the ability to regulate the output voltage to a reference chosen by the user (12V or 24).

Figure 6.a shows the desired PV voltage properly provided by RCC MPPT algorithm.

Figure 6.b shows the PV voltage properly following its reference when the irradiation and temperature are constant.

Figure 7.c illustrates the maximum power extracted from the solar panel according to a solar radiation and temperature (1045 w).

Figure 7.d shows that the output voltage well achieved to its reference (12 to 24v).

Figure 7.e illustrate a zoom of the output voltage. When the desired voltage change from 12V to 24V at time t= 3s, the output voltage

reaches the reference voltage after 50ms and is kept there until the end of simulation.

These simulations show the effectiveness of the combination of backstepping controller approach and RCC MPPT to search the maximum power and ability of the for the adjustment of the output voltage.

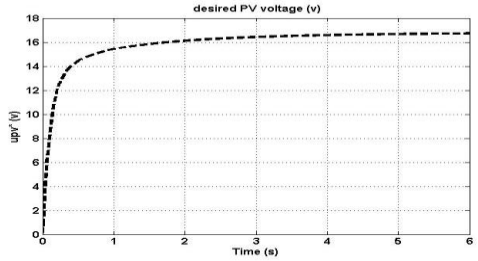

(a)

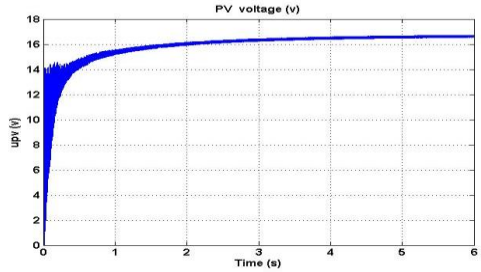

(b)

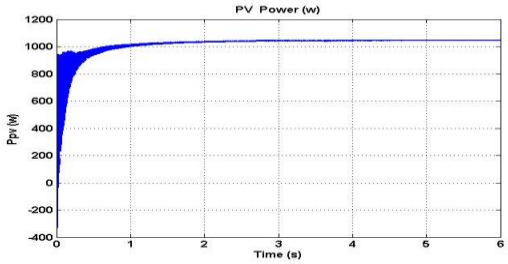

(c)

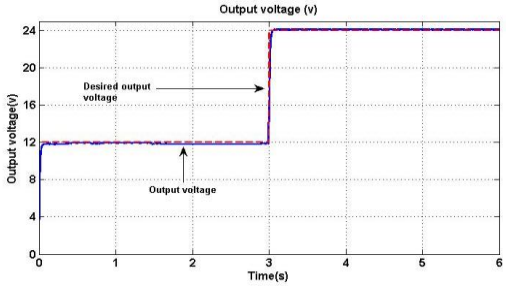

(d)

Figure.6. (a) radiation, (b) Temperature, (c) Load torque, (d) PV voltage, (e) PV power, (f) DC voltage

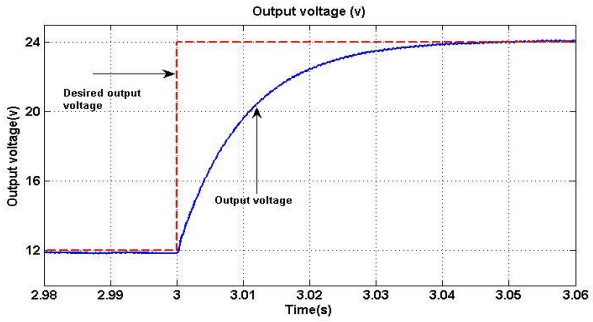

(e)

Figure.7. (a) Desired PV voltage, (b) PV voltage, (c) PV power (d) Output voltage and reference, (e) Zoom of the output voltage [2.98 to 3.06s]

5 Conclusion

A backstepping control strategy has been developed for a solar generating system to extract the power from a photovoltaic panel and adjust the output voltage to reference. A desired array voltage is designed online using a RCC MPPT searching algorithm to seek the unknown optimal array voltage. To track the designed trajectory, a tracking controller is developed to search reference of PV voltage of the boost converter. The proposed controller is proven to yield global asymptotic stability with respect to the tracking errors via Lyapunov analysis. Simulation results prove the robustness of the nonlinear controller with respect the desired output voltage change.

References:

[1] Casadei, D., Grandi, G., Rossi, C. , Single-phase single-stage photovoltaic generation system based on a ripple correlation control maximum power point tracking, IEEE Transactions on Energy Conversion, 2006

[2] Liu, S., Liu, H., Zhao, Y., A solar maximum power point tracking algorithm based on discrete-time ripple correlation control, Nongye Gongcheng Xuebao/Transactions of the Chinese Society of Agricultural Engineering, 2013

[3] Lalouni, S., Rekioua, D. ,Modeling and simulation of a photovoltaic system using fuzzy logic controller, Proceedings - International Conference on Developments in eSystems Engineering, 2009, pp.. 23 - 28

[4] Barth, C., Pilawa-Podgurski, R.C.N. ,Dithering digital ripple correlation control for photovoltaic maximum power point tracking , IEEE Power and Energy Conference at Illinois, PECI 2013

[5] Rekioua, D., Matagne, E. ,Optimization of photovoltaic power systems: Modelization, Simulation and Control Green Energy and Technology, ,2012